Waste Management 166 (2023) 270–279

Contents lists available at ScienceDirect

Waste Management

journal homepage: www.elsevier.com/locate/wasman

Ce/Pumice and Ni/Pumice as heterogeneous catalysts for syngas production from biomass gasification

S. Señorans, J. R-Díaz, D. Escalante, L.A. González, L. Díaz *

Chemical Engineering Department, University of La Laguna, Avda. Astrofísico Fco. Sánchez s/n, La Laguna, Tenerife, Canary Island 38200, Spain

ARTICLE INFO

Keywords:
Heterogeneous catalyst
Gasification
Syngas
Biomass
Pumice
Pennisetum setaceum

ABSTRACT

This work presents a study of synthesis and characterization of catalysts-based cerium and nickel supported on the pumice stone (Ce/Pumice and Ni/Pumice) to be used in the gasification process of an invasive species present in the Canary Islands, such as *Pennisetum setaceum* to obtain syngas. Specifically, the effect of the metal impregnated on the pumice, and the effect of catalyst on the gasification process was studied. For this purpose, the composition of the gas was determined and the results obtained were compared with those obtained in non-catalytic thermochemical processes. Gasification tests were performed using a simultaneous thermal analyzer coupled with a mass spectrometer, providing a detailed analysis of the gases released during the process. The results showed that during the catalytic gasification process of the *Pennisetum setaceum*, the gases produced appear at lower temperatures in the catalytic process that in the non-catalytic process. Specifically, H_2 appears at 640.42 °C and 641.84 °C when Ce/pumice and Ni/pumice were used as catalyst, respectively, compared to 697.41 °C for the non-catalytic process. Moreover, the reactivity at 50 % of char conversion for the catalytic process (0.34 and 0.38 min^{-1} for Ce/pumice and Ni/pumice, respectively) was higher than for the non-catalytic process (0.28 min^{-1}), indicating that the incorporation of Ce and Ni on the pumitic material increases the gasification rate of the char compared to the pumitic support. Catalytic biomass gasification is an innovative technology that can provide new opportunities for research and development of renewable energy technologies, as well as for the creation of green jobs.

1. Introduction

The increase in the world's population and the development of current production and consumption systems mean that large quantities of energy are needed. These energy supplies come mainly from fossil fuels (coal, oil, gas); translating into a high energy dependence through which its excessive use will end up causing the depletion of its reserves. For this reason, renewable resources based on low-carbon sustainable technologies such as solar, wind, geothermal, hydroelectric and biomass are today possible alternative and highly attractive sources of energy for sustainable development. Emphasis is placed on more sustainable and renewable sources of energy derived from biomass, such as agro-industrial derivatives that are used to produce biofuels (Maurya et al., 2023). Biomass is the only renewable carbon source for biofuel production and the only available alternative that can be quickly introduced into the biofuel market matrix. Biomass energy is very low in sulfur, nitrogen and ash, thus generating lower emissions of sulfur dioxide (SO_2), nitrogen oxides (NO_x) and soot than conventional fossil fuels (Mujtaba et al., 2023). In addition, zero net carbon dioxide (CO_2) emissions can be achieved thanks to the photosynthesis process carried out by plants.

There are different sources of biomass depending on their origin for obtaining energy, such as natural, residual, marine, surplus agricultural crops and energy crops, and within this classification is lignocellulosic biomass, which is an important source of renewable energy with great potential in the production of biofuels, cogeneration of electrical energy and generation of chemical compounds, among other applications (Murillo and Galán, 2020). Lignocellulosic biomass is not part of the human food chain and therefore its use for energy production is not a threat to the global food supply (Singh et al., 2023); it is mainly composed of hemicellulose, cellulose, lignin and contains a variety of minor components (inorganic matters).

One of the biomasses that can be valorized energetically are invasive plants. In this work, the energy recovery of an invasive species, *Pennisetum setaceum*, was chosen for this study because of its local abundance, low supply cost and unresolved environmental problems. The species

* Corresponding author.
E-mail address: laudiaz@ull.edu.es (L. Díaz).

https://doi.org/10.1016/j.wasman.2023.05.017
Received 22 January 2023; Received in revised form 27 April 2023; Accepted 9 May 2023

Pennisetum setaceum (common name "fountain grass") is included in the Spanish Catalogue of Invasive Alien Species (Royal Decree 630/2013 of 2 August). The massive expansion of this invasive species in the ecosystems of the Canary Islands generates a high environmental impact. At present, the only measure adopted by public institutions is its collection and disposal as waste in landfills. Therefore, its collection and possible energy recovery would be an interesting solution, as well as protecting the endemic and autochthonous elements of the local flora.

Biomass, as a renewable energy source, can be exploited directly or through thermochemical or biochemical processes to obtain electrical, thermal or chemical energy (Manikandan et al., 2023). Among all the thermochemical conversion processes (combustion, pyrolysis and gasification) gasification is considered as one of the most suitable for the efficient transformation of solid biomass into syngas (H_2 + CO) which can be used for heating or further synthesis of chemicals or liquid fuels (Khan et al., 2022). Gasification is a partial oxidation of solid biomass that works at high temperatures (900–1400 °C) (Arias, 2018). Tulu et al. (2002) studied the kinetic modeling of biomass gasification in bubbling fluidized bed gasifiers and optimization methods to maximize gasification products. The authors showed that an increase in temperature, from 650 °C to 850 °C. promoted H_2 production from 18.73 % to 36.87 %. However, in recent years the use of catalytic biomass gasification has been studied due to the disadvantages of working at such high temperatures and the formation of undesired products such as tars. The presence of catalyst can reduce the activation energy of some reactions, it can increase the content of H_2 in syngas and remove the by-product tars (Hu et al., 2021).

The catalysts used in biomass gasification are usually based on alkali metals, transition metals, and natural minerals. However, alkali metals such as Na and K are easy to be evaporated causing problems such as particle agglomeration, catalyst activity lost and recovery difficulties (Hernández, 2019; Ren et al., 2019). Natural minerals, such as olivine, sepiolite, dolomite and limonite have been used as catalyst for biomass gasification due to the presence of metal oxides (Al_2O_3, F_2O_3, MgO, CaO) which have shown some efficiency for tar conversion (Kumar Ghodke et al., 2023; Liu et al., 2023; Swierczynski et al., 2007). On the other one, Ni-based catalysts have been shown to be the most effective in catalytic destruction of tar. The use of Fe or Co is also widespread (Hu et al., 2021; Çakan et al., 2022). These catalysts are most widely used due to its high activity, low cost and easy regeneration (Zhang et al., 2018). Specifically, several studies have shown that the use of Ni supported on natural materials such as dolomite, sepiolite and olivine in fluidized bed reactors are good catalysts for biomass gasification due to their great capacity for reforming, they are also very active in removal of tars (Hernández, 2019).

In this study, *Pennisetum setaceum* was used as biomass to carry out the catalytic gasification process using metals supported on pumice (Ni/Pumice and Ce/Pumice). Specifically, the synthesis of these catalysts and their physical–chemical characterization was carried out. In addition, the main evolved gases in the thermochemical process were analysed when the process was carried out without catalyst, with Ce/Pumice and Ni/Pumice as catalyst, and with the support material (pumice). All this to know the effect of the type of metal impregnated on the pumice, and the introduction of the catalyst in the thermochemical process.

Catalytic biomass gasification is a promising technology for renewable and sustainable energy production that can contribute to several Sustainable Development Goals (SDGs): Affordable and Clean Energy (SDG 7), Industry, innovation and infrastructure (SDG 9) and Climate Action (SDG 13). Specifically, catalytic biomass gasification can produce syngas can be used to generate electricity and heat in a sustainable and clean way. Furthermore, catalytic gasification of biomass can reduce dependence on fossil fuels. It is an innovative technology that can provide new opportunities for research and development of renewable energy technologies, as well as for the creation of green jobs. This thermochemical process reduces greenhouse gas emissions by producing energy and chemicals from renewable biomass instead of non-renewable fossil fuels.

2. Experimental

2.1. Biomass

Pennisetum Setaseum (PS) samples were obtained from Tenerife (Canary Islands). PS samples were cut and dried in the oven at 70 °C for 24 h to facilitate grinding. After drying, the material was ground in a planetary ball mill (Pulverisette 6, Fritsch) and sieved. The fraction below 500 μm was selected.

2.2. Catalyst synthesis

A cerium and a nickel catalyst were synthesized on pumice stone (catalytic support), with 5 % by weight of the metal on the support. For this, pumice stone particles (Panreac) with a size between 1.4 and 3.0 mm were used. The modification of the support material was carried out by the wet impregnation method using cerium (III) nitrate hexahydrate (Acros Organics, 99.5 %) and nickel (II) nitrate hexahydrate (Labkem, 98 %) as precursors. For this, approximately 30 g of pumice were ground in a mortar, then the pumice was sieved and the fraction between 200 and 400 μm was selected. Next, solutions of cerium nitrate and nickel nitrate in water were prepared. Then, the grams of pumice stone were introduced into porcelain capsules and the solutions of cerium nitrate and nickel nitrate previously prepared were added. They were dried in an oven at 100 °C overnight and finally calcined at 800 °C for 2 h. The synthesized materials were designated as Ce/Pumice and Ni/Pumice.

2.3. Catalyst characterization

The N_2 adsorption isotherms studies were performed using Micromeritics Instruments, ASAP 2020, at −196 °C, with liquid nitrogen to reach the measurement temperatures. Surface area and total pore volume of the samples were calculated applying the Brunauer-Emmett-Teller (BET) method in the range from 0.05 to 0.3. Previously, the samples were degassed at 250 °C for 16 h. The presence of functional groups of the pumice materials was determined by Fourier transform infrared spectrometer (FTIR) using an Agilent Cary 630 spectrometer with the attenuated total reflectance (ATR) accessory (ZnSe). FTIR spectra were recorded in the wavenumber range of 4000–500 cm^{-1} and, for each spectrum, 32 scans were accumulated at a spectral resolution of 4 cm^{-1}. The instrument was purged with nitrogen before the measurements and all FTIR measurements were carried out at room temperature. A Panalytical X'Pert Pro powder diffractometer with X'Celerator detector was used to determine the crystalline structure of the materials, using Cu Kα 1.2 radiation with an intensity of 40 mA and a potential of 45 KV. The diffractograms were carried out in the 2θ range between 4 and 80°. The analysis on mineral matter content in each sample was performed using Energy-Dispersive X-ray Fluorescence (EDXRF) spectrometer, model Bruker S2-Puma (50 W). The thermogravimetric analysis was carried out in a simultaneous thermal analyzer (Discovery SDT 650) with a DSC/TGA system that offers simultaneous heat flow and weight data in real time that allows the identification, purity control and stability of the materials. A 90 μL alumina crucible and a temperature program of 10 °C/min^{-1} were used, from room temperature to 1000 °C with a fed gas flow rate of 50 mL·min^{-1} of N_2. Approximately 10 mg of the sample were used for the analyses.

2.4. Gasification of the Pennisetum Setaseum

The non-catalytic and catalytic gasification of the *Pennisetum Setaseum* was carried out in the simultaneous thermal analyser SDT650 (TA Instruments). The gases released from the gasification process were analysed by mass spectrometry (MS). For this, a mass spectrometer,

ThermoStar GSD301-T2 with a quadrupole mass analyser and an ionization potential of 70 eV from Pffeifer Vacuum, was coupled to the thermal analyser (Fig. 1). The connection line between the equipment was made by means of an inert capillary tube, heated to avoid condensation of the less volatile products, which carries part of the gases released in the thermal analyser to the ionization chamber of the mass spectrometer.

The experiments performed were designated as follows: non-catalytic gasification of *Pennisetum Setaseum* (PS), catalytic gasification with Pumice (PS + P), with Ce/Pumice (PS + Ce/P) and with Ni/Pumice (PS + Ni/P). For catalytic gasification runs, 10 % by weight of catalyst with respect to biomass weight was employed. 12 mg sample was used for each experiment. A precision balance was used to weigh the biomass and the catalyst. Both were mixed with a mini vortex mixer. More details on the experiments can be found in Table S1 (Supplementary material). All experiments were performed in triplicate, which were averaged. The gasification process was carried out in two stages. In the first stage, the samples (~10 – 13 mg) were pyrolyzed at 40 °C min^{-1} up to 900 °C after placing them in open alumina crucibles under an inert atmosphere and 50 mL min^{-1} flowing nitrogen. In the second stage, the sample obtained in the pyrolysis process was subsequently gasified in air, in isothermal conditions at 900 °C for one hour. The analysis conditions of each stage are: 1) Analysis conditions for the first stage of gasification (referred to as pyrolysis): initial temperature: room temperature, final temperature: 900 °C, sample amount: 12 mg, heating rate: 40 °C min^{-1}, atmosphere: nitrogen, gas flow: 50 mL min^{-1}, crucible type: alumina. 2) Analysis conditions for the second stage of gasification: initial temperature: 900 °C, final temperature: 900 °C, time: 60 min, atmosphere: air, gas flow: 50 mL min^{-1}, crucible type: alumina.

2.5. Analytical methods

The main properties of biomass as fuel were analyzed. Proximate analysis was performed according to standards analytical methods UNE-EN ISO 18134:2016, UNE-EN ISO 18122:2016, UNE-EN ISO 18123:2016, for moisture content (MC), ash content (AC) and volatile matter (VM), respectively. The fixed carbon (FC) was calculated by subtracting ash and volatile matter contents from 100 % (in a dry basis). Ultimate analysis was used to determine the concentration of carbon, hydrogen, nitrogen, oxygen and sulphur content of the biomass samples. The chemical composition was obtained by CHNS elemental analysis using FlashEA 1112 Organic Elemental Analyzer. The oxygen content was estimated by subtraction. Empirical correlation has been used for calculating the higher heating value (HHV) from the values obtained in the proximate analysis, proposed by Channiwala and Parikh (Channiwala and Parikh, 2002). Moreover, the lower heating value (LHV) was determined from the HHV considering the content of hydrogen and moisture in the biomass and 2260 kJ kg^{-1} as latent heat of vaporization (Basu, 2010). The skeletal density of the samples was measured by gas pycnometry (Micromeritics Instruments, Accupyc 1330) using a 3.5 cm^3 sample module and helium as filling gas (99.995 % pure). All analyses were performed in triplicate.

Besides, gases from the gasification process were continuously collected during the decomposition steps and then analysed through mass spectrometry. In mass spectrometry, the mass/charge ratios of the emission of compounds during gasification were examined, paying special attention to the search for gases with energy potential emitted in the thermal use of biomass. Specifically, the target signals with *m/z* ratios of 2, 15, 18 and 44 were focused on detecting H_2, CH_4, H_2O and CO_2 evolution. The evolution of CO is not shown since the *m/z* ratio of the carrier gas (N_2) does not allow its accurate detection.

2.6. Char conversion, reactivity and gasification rate

Char conversion, reactivity and gasification rate were determined to characterise the gasification process. The char conversion (x_i) represents the weight loss fraction or mass conversion ratio, and it was calculated according to the Eq. (1) (Parascanu et al., 2017):

$$x_i = \frac{w_0 - w_i}{w_0 - w_f} \quad (1)$$

where w_0 is the initial mass of the char sample at time t_0, w_i is the mass of the char sample at time t and w_f is the final mass of the char sample. The char reactivity (R_i) is dependent on the temperature and gas composition and varies with the conversion degree. Therefore, a representative value of reactivity is needed to make reliable comparisons. In this work, the reactivity at 50 % of char conversion (R_{50}) was representative of the gasification process. The reactivity of char was calculated by the Eq. (2) (Parascanu et al., 2017):

$$R_i = -\frac{1}{w_i}\cdot\frac{dw_i}{dt} = \frac{1}{1-x_i}\cdot\frac{dx_i}{dt} \quad (2)$$

where x_i and w_i are the conversion and mass of char at any time, respectively. The gasification rate (r_i) was also used to describe the gasification reaction and was defined as follows (Eq. (3)) (Parascanu et al., 2017):

$$r_i = \frac{dx_i}{dt} \quad (3)$$

3. Results and discussion

3.1. Biomass characterization

The proximate analysis, ultimate analysis, heating power and density of *Pennisetum Setaseum* are shown in Table 1. Proximity analysis provides an indication of the quality of the biomass to be converted into energy. Feedstocks with low moisture content (less than 50 wt%) are required for thermochemical conversion processes. A high moisture content reduces the calorific value of the fuel and adversely affects the overall energy balance of the conversion process as a result of the drying processes (López-González et al., 2013). The results from Table 1 show that *Penisetum setaceum* is characterized by relatively low moisture content, 11.79 wt%. Manić et al. (2019) found similar moisture contents in several agricultural residues: 8.58 wt%, 11.63 wt% and 9.27 wt% for corn brakes, wheat straw and hazelnut shell, respectively.

In addition, *Penisetum setaceum* contains 15.41 wt% of ash, 72.79 wt

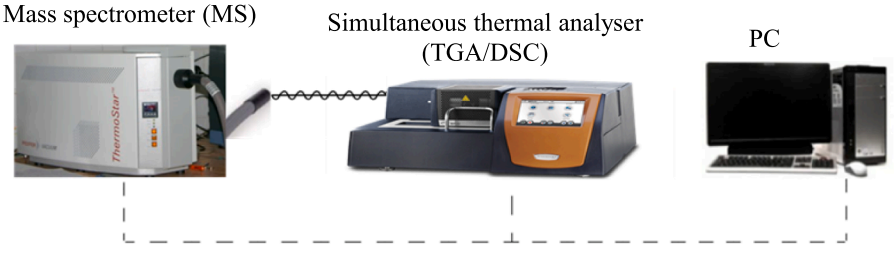

Fig. 1. Schematic diagram of the biomass catalytic gasification system.

Table 1
Biomass characterization.

Proximate analysis (wt%)		Ultimate analysis (wt%)	
Moisture content	11.79	C	38.87
Ash content	15.41	H	5.06
Volatile matter	72.79	N	0.62
Fixed carbon	11.80	S	0.03
		Ashes	15.41
		O	40.01
Heating power		**Density**	
HHV (MJ kg^{-1})	15.1	Density (kg m^{-3})	1517.5
LHV (MJ kg^{-1})	13.8		

% of volatile matter and 11.80 wt% of fixed carbon. It is appropriate that biomasses subjected to thermochemical processes have a low ash content and a high volatile matter content. A high ash content can lead severe agglomeration, fouling and corrosion in boilers or gasifiers (Mettanant et al., 2009); however, the main problems caused by ashes (erosion, deposit formation) are conditioned more than by their quantity, by their composition, especially if they contain alkali metals such as potassium or halides such as chlorine (Basu, 2010). The fixed carbon content of the biomass is in the range of those found for wood (12.28–29.90 wt%) (García et al., 2012).

The ultimate analysis for *Penisetum setaceum* is also reported in Table 1. Carbon and oxygen are the majority elements with 38.87 wt% and 40.01 wt%, respectively. The carbon, hydrogen and oxygen content of feedstocks used in thermochemical processes is beneficial, in contrast to sulfur and nitrogen, as they can be sources of polluting emissions. High sulfur content could release SO_2 and H_2S in the gaseous product during the thermochemical process. The sulfur content in biofuels generates SO_2 that forms sulfates, which can condense in the heat exchanger walls or generate ashes. Therefore, low levels of S in the feedstock are required (García et al., 2012). *Penisetum setaceum* has a relatively low sulphur content (0.03 wt%). In addition, the nitrogen content is also low (0.62 wt%). Similar values were found by García et al. (2012) when analyzing the N content of more than 200 biomass samples. The low percentage of N present in the biomasses indicates that its contribution to NO_x in waste gases is lower than from the air, which has a contribution nearly 15 or 20 times higher.

In addition, biomass density and heating values have also an impact on the behaviour of thermochemical conversion processes. The heating value of a material is an indicator of its content in energy released when it burns in the air. Commonly, biomass is characterized by HHV of 15–20 MJ kg^{-1}, which is much lower than that of coal varying from 22 to 35 MJ kg^{-1} (Channiwala and Parikh, 2002; Neves et al., 2011). *Penisetum setaceum* contains a HHV of 15.1 MJ kg^{-1}. The difference between the HHV and LHV values is not considerable, so the removal of heat from vaporization does not greatly influence the results. Dense particles contribute to a longer burnout time; conversely, low-density particles have lower energy efficiency, also lead to high transport costs and reduce the storage capacity of both the biomass producer and the end-user (Obernberger and Thek, 2004). The density value of *Penisetum setaceum* (1517.5 kg m^{-3}) is in the range of those found by Parascanu et al. (2017) when they analyzed different Mexican biomasses (Castor bean peel, Castor bean stem, *Agave bagasse*, Coffee pulp, *Opuntia stem* and *Pinus sawdust)* by the same method (1346.3–1726.7 kg m^{-3}). Penisetum *setaceum* it turns out to be a suitable feedstock for thermochemical processes.

3.2. Catalyst characterization

The BET Surface (S_{BET}) and the mean pore diameter of the pumitic materials are shown in Table S2 (Supplementary material). All the isotherms exhibited type IV isotherms in IUPAC classification, indicating that the materials are mesoporous solids. Mesopores can provide abundant reaction centers, which is beneficial to the contact between tar and active sites (Wang et al, 2022). It is observed that the value of the BET surface increases with the impregnation of the metal, obtaining the largest BET surface for the Ce/Pumice catalyst. Regarding the average pore diameters, it is confirmed that all materials are mesoporous since they are in the range 2 and 50 nm. Moreover, it is observed that both, the S_{BET} and the mean pore diameter, are greater for the Ce/Pumice material than for the Ni/Pumice and Pumice.

The FTIR spectrum of the Pumice, Ce/Pumice and Ni/Pumice are displayed in Fig. 2a. The characteristic bands observed in the FTIR spectra are typical of aluminosilicates. The broad band located between 600 and 1200 cm^{-1} is attributed to the internal vibration of the TO_4

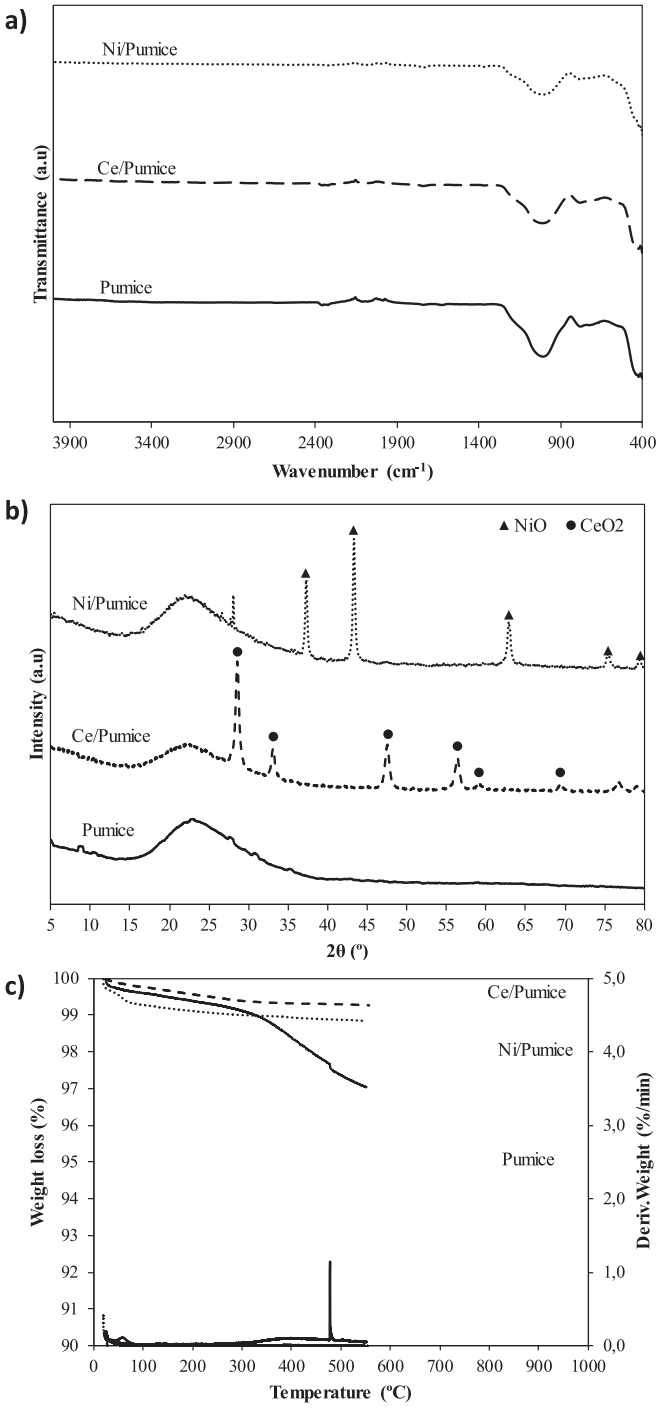

Fig. 2. a) FTIR spectra, b) XRD patterns. and c) TGA-DTG curves of the pumitic materials.

tetrahedra (T = Al or Si) (Díaz, 2018). The wide range of this band is attributed mainly to the amorphous nature of the pumice, as well as to the short-range ordering of the Si and Al tetrahedra (Rodríguez Martínez, 2009). The greater intensity of the main peak of the Pumice with respect to that of the impregnated materials can be associated with the greater number of tetrahedrons present in the material.

Fig. 2b shows the X-ray diffraction patterns of each of the pumitic materials. There is an absence of crystallinity in the support material (pumice) since no peaks are observed in its XRD pattern. In the range of 2θ = 20°-30° a broad peak typical of amorphous aluminosilicates is observed, specifically characteristic of the amorphous silica structure (SiO_2), an oxide found in large quantities in pumitic materials (Temuujin et al., 2002). However, the impregnation of pumice with cerium and nickel generated crystallinity in the materials. As shown by their diffraction patterns, cerium and nickel are in the form of oxides. In addition, XRD pattern of Ni/Pumice (Fig. 2b) a peak at 2θ = 27.5° corresponding to phillipsite, which is a kind of natural zeolite. This type of zeolite is usually found in pumitic materials (Borges et al., 2011).

In order to corroborate the metal incorporation on the surface of the impregnated pumitic materials, an X-ray fluorescence analysis was performed. Table S2 shows that Si and Al were the metals present in the highest quantity in all the materials, with an average percentage of 57.7 % and 10.6 % for Si and Al, respectively. Pumice is an aluminosilicate, so its main components are Si and Al. In addition, all materials exhibited a significant percentage of K (average value of 8.7 %), this is since metals such as K or the Na compensating the charges of the tetrahedra (TO_4) (Díaz, 2018). Absence of cerium and nickel was observed in Pumice and their appearance in the new synthesized materials indicated that the metals were deposited on the surface of the pumice in a satisfactory way.

TGA was employed to study the thermal stability of the materials as a function of temperature. Fig. 2c shows that the materials are thermally stable, with mass losses of less than 5 % by weight for Pumice and less than 1 % by weight for Ce/Pumice and Ni/Pumice. The mass loss for the Pumice occurs in a staggered manner, with two more pronounced sections corresponding to two peaks detected in the DTG curve. The first peak at a temperature of 478 °C and the next at 644 °C, these may be due to the presence of occluded water in the material, because the pumice is not calcined previously. The catalysts Ni/Pumice and Ce/Pumice have a high thermal stability. In the synthesis process they were subjected to calcination up to 800 °C, so the water occluded in the pumice pores was removed during the synthesis. The small loss of mass observed (less than 1 % by weight) could be attributed to physisorbed water on the surface because of the oxides formed.

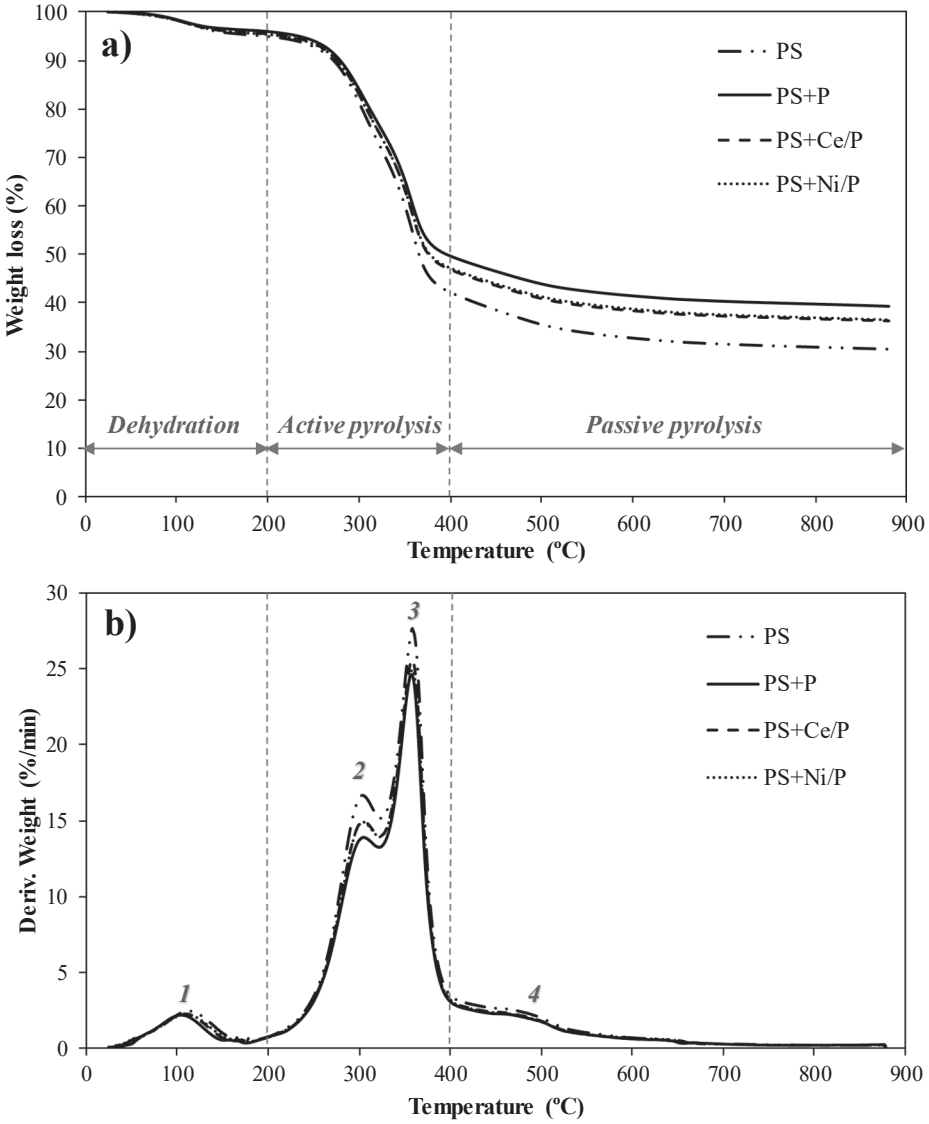

Fig. 3. TGA (a) and DTG (b) curves of the first gasification stage.

3.3. Gasification process

To investigate the energy recovery of the biomass used, the gasification of *Pennisetum setaceum* (PS) was initially conducted and the results obtained were subsequently compared with the gasification of this biomass by incorporating of the catalyst (PS + P, PS + Ce/P, PS + Ni/P), thus obtaining the effect of the catalysts on the gasification process. Fig. 3a) and Fig. 3b) shown the weight loss (TGA curve) and the rate of weight loss (DTG curve) versus temperature, respectively, during the first stage of gasification process, of the four experiments conducted. This first stage of gasification process involves drying the biomass and pyrolysis. In addition, table 2 summarizes the characteristic parameters obtained from the TG/DTG curves of the first gasification stage: the temperature range (T), the percentage of mass loss (w), the maximum of the DTG curve (DTG_{max}) and its corresponding temperature (T_{DTGmax}) are specified. As illustrated in Fig. 3, the thermal decomposition process of the samples allows to distinguish three differentiated zones (zone I: dehydration, zone II: active pyrolysis and zone III: passive pyrolysis), characteristic of the pyrolysis process in lignocellulosic biomass. What happens in each of the zones is described below. The first zone (dehydration) occurred below 200 °C, which corresponds to dehydration of *Penisetum setaceum*, where biomass absorbs heat, releasing moisture from the samples in the form of water vapor. It can be observed that the differences between the use or not of the catalyst in weight loss are not significant and are in a range between 4.05 and 5.06 %. In DTG curves, a weak peak appeared around 104–113 °C (peak 1).

The second zone (active pyrolysis), occurred in the temperature range of 200–400 °C, is the devolatilization process, which is the main decomposition process. In this zone, several volatile components were released gradually, resulting in a large mass loss. Moreover, in this temperature range two decomposition processes occur, coinciding with peaks 2 and 3 according to the DTG curves (Fig. 3 b). The first occurs between 200 °C and 330 °C, which can be attributed to the reaction of hemicellulose decomposition (peak 2) (Yang et al., 2007), reaching T_{DTGmax} at a temperature of around 304 °C (Table 2). Whereas the second process happens between 330 °C and 400 °C and corresponds to the decomposition of cellulose (peak 3) (Yang et al., 2007); the T_{DTGmax} is around 358 °C (Table 2). The decomposition of these materials (hemicellulose, cellulose) reverts to the production of a significant fraction of carbonized solid waste (char).

In the third zone (passive pyrolysis), the char oxidizes. Above 400 °C, weight losses continue to occur (8–9 %), which corresponds to the decomposition of lignin, which begins in zone II and takes place slowly. T_{DTGmax} is achieved at a temperature around 480 °C (peak 4) (Table 2).

Fig. 3a) shows a greater loss of weight in the pyrolysis process of the fountain grass (PS); this is because in the catalytic pyrolysis process (PS + P, PS + Ce/P and PS + Ni/P), once the thermal decomposition of the biomass has occurred, the catalyst will remain present (inorganic material with high thermal stability). In addition, if the catalytic pyrolysis processes are carried out, a greater loss of weight is observed when Ce/Pumice and Ni/Pumice catalysts are used, indicating that these catalysts can accelerate the decomposition of the hemicellulose, cellulose and lignin contained in the fountain grass, faster that when Pumice is used. Then, if the pyrolysis process is compared (Fig. 3), it is observed that thermal decomposition occurs in the following decreasing order PS < PS + Ni/P ≈ PS + Ce/P < PS + P. At temperatures above 600 °C, the generated char is increased when a catalyst is introduced into the gasification process compared to the non-catalytic process (PS) and can therefore be recovered in this first gasification stage.

The possible gases produced in the different experiments were analyzed, using mass spectrometry, according to their mass/charge (m/z) ratios as observed in Fig. 4. Although several species were detected during pyrolysis such as aldehydes, ketones, acids, alkanes, alcohols and esters, the intensities of the main species were discussed. Specifically, Fig. 4 illustrated ion current curves monitored using MS for H_2 ($m/z = 2$), CH_4 ($m/z = 15$), H_2O ($m/z = 18$) and CO_2 ($m/z = 44$), respectively, during the first gasification stage of *Pennisetum setaceum*. It is also known that CO release occurs during cracking of the structures and secondary reactions; but the m/z ratio of the carrier gas (N_2) does not allow the precise detection of CO evolution (Özsin and Pütün, 2017). The vertical dashed lines in the Fig. 4 indicate the maximum temperatures for the experiment performed with the Ce/Pumice catalyst. Moreover, in table 3 maximum temperatures of the peaks detected in the ion current curves monitored using MS corresponding to the gases H_2, CH_4, H_2O and CO_2 are shown. By comparing the ion current curves of the gases for the first gasification stage of PS, PS + P, PS + Ni/P and PS + Ce/P experiments, the maximum temperature of the peaks detected, for all m/z, when a catalyst is introduced in the process moves to the low-temperature direction, which is advantageous. Specifically, the appearance of the high-temperature peaks occurs in the following decreasing order: PS + Ce/P > PS + Ni/P > PS + P > PS; that is, when Ce/Pumice is used as a catalyst, the production of gases such as H_2, CO_2, CH_4 and H_2 appear at lower temperatures than in the other experiments, as shown in the Table 3 and Fig. 4. Gases appear at the highest temperatures when no catalyst is introduced into the thermochemical process (Table 3 and Fig. 4). For example, the temperatures at which maximum peaks appear on the ion current curve for hydrogen are 640.42 °C (peak 1) and 733.44 °C (peak 2) when the Ce/Pumice catalyst is used; however, when no catalyst is introduced into the process, the temperatures at which the maximum peaks appear are raised, 697.41 °C (peak 1) and 771.81 °C (peak 2), respectively. These results demonstrate the catalytic action of pumitic materials on the thermal decomposition process of biomass because they reduce the activation energy of the reactions that occur.

In addition, the effect of impregnation of the metal on the pumice stone is also evident. The temperatures at which maximum peaks appear on the ion current curves for all analyzed gases are for all gases analyzed, they are higher with Pumice than with Ni/Pumice and Ce/Pumice. In turn, the temperatures at which maximum peaks appear are higher with the Ni/Pumice catalyst than with the Ce/Pumice. This can be attributed to the S_{BET} and the mean pore diameter are greater for the Ce/Pumice catalyst than for the Ni/Pumice and Pumice (Table S2). Therefore, this reflects that the greater the S_{BET} and the greater the mesoporosity of the material, the greater the reduction in the activation energy of the reactions and, therefore, the generation of gases occurs at a lower temperature.

Catalysts can be used to enhance the reactions involved in gasification. Many gasifiers must operate at high temperatures so that the gasification reactions will proceed at reasonable rates. Unfortunately,

Table 2
Temperature ranges (°C) and weight loss (%) of the first gasification stage.

		PS	PS + P	PS + Ce/P	PS + Ni/P
		Zone I. Dehydration			
1	**T(°C)**	25–200			
	w (%)	5.06	4.05	4.54	4.67
	DTG_{max} (%/min)	2.46	2.20	2.27	2.25
	T_{DTGmax} (°C)	112.94	104.23	108.34	110.02
		Zone II. Active pyrolysis			
2	**T(°C)**	200–330			
	w (%)	25.36	22.05	23.26	23.13
	DTG_{max} (%/min)	16.67	13.90	14.97	14.91
	T_{DTGmax} (°C)	303.97	304.83	304.85	304.06
3	**T(°C)**	330–400			
	w (%)	27.44	24.27	25.38	25.05
	DTG_{max} (%/min)	27.66	24.63	25.61	24.94
	T_{DTGmax} (°C)	358.63	357.49	358.17	358.27
		Zone III. Passive pyrolysis			
4	**T(°C)**	400–600			
	w (%)	9.44	8.22	8.48	8.43
	DTG_{max} (%/min)	3.52	3.08	3.20	3.18
	T_{DTGmax} (°C)	482.87	480.99	480.01	480.07
		Residue remaining after the first stage of gasification			
	T(°C)	greater than 600			
	w (%)	30.42	39.27	36.26	36.47

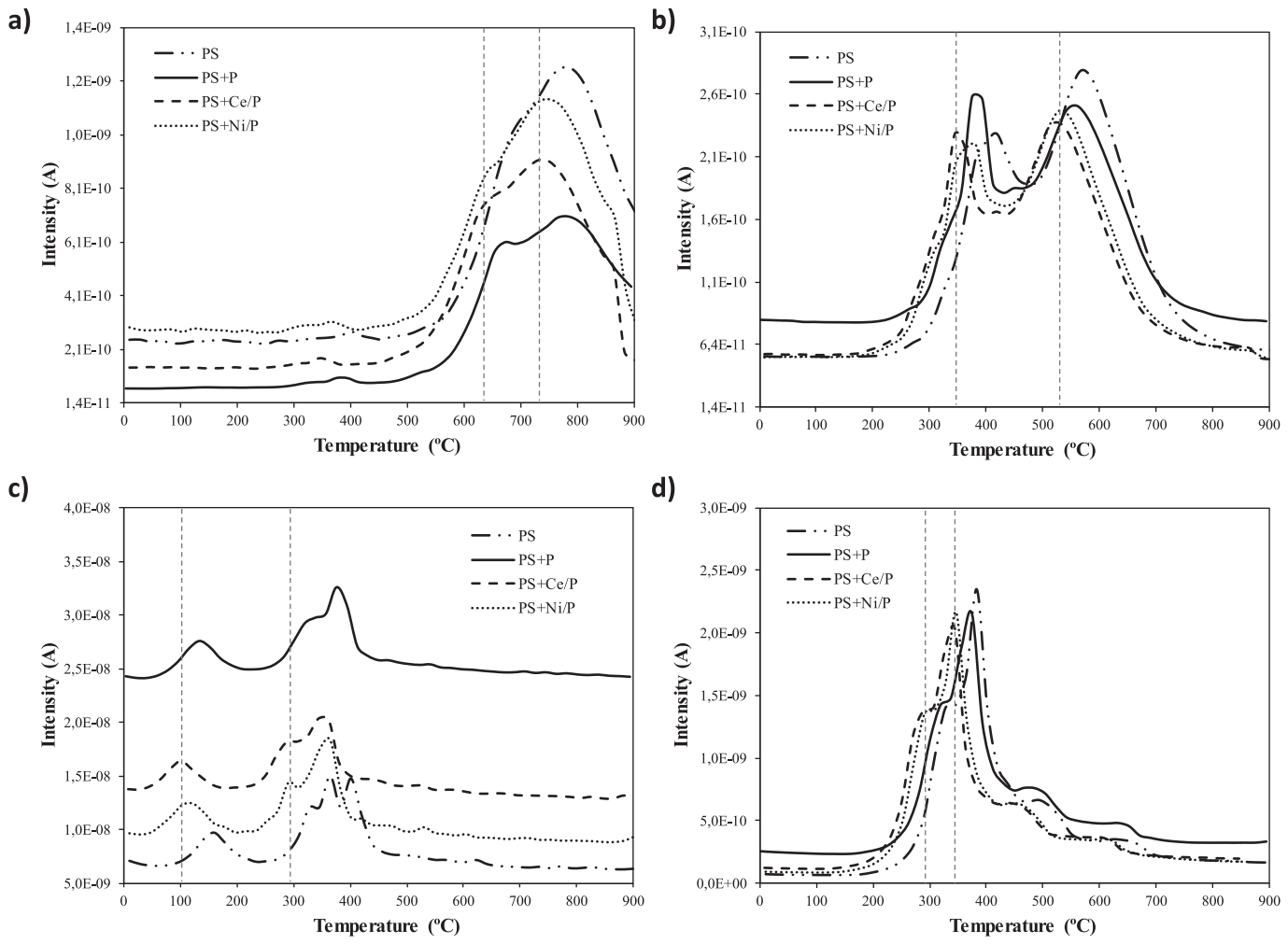

Fig. 4. Ion current curves monitored using MS for a) H_2 ($m/z = 2$), b) CH_4 ($m/z = 15$), c) H_2O ($m/z = 18$) and d) CO_2 ($m/z = 44$) during first gasification stage.

Table 3
Maximum temperatures of the peaks detected in the ion current curves corresponding to the gases H_2, CH_4, H_2O and CO_2.

		Experiment			
		PS	**PS + P**	**PS + Ce/P**	**PS + Ni/P**
H_2	Peak 1	697.41	671.28	640.42	641.84
$m/z = 2$	Peak 2	771.81	764.23	733.44	735.00
CH_4	Peak 1	400.94	375.32	344.61	364.21
$m/z = 15$	Peak 2	567.32	559.98	510.63	530.39
H_2O	Peak 1	159.14	133.23	102.30	102.96
$m/z = 18$	Peak 2	327.06	319.83	289.15	290.19
CO_2	Peak 1	327.07	319.83	289.15	290.19
$m/z = 44$	Peak 2	382.57	375.32	344.61	345.76

high temperatures can sometimes necessitate special materials, extra energy input, and cause efficiency losses if heat cannot be reclaimed. The use of catalysts such as Ce/Pumice and Ni/Pumice would reduce the operating temperatures of a gasifier. In addition, the catalysts presented high thermal stability (Fig. 2c) and are low-cost catalysts since the support used (pumice stone) is a volcanic, natural and cheap material.

In the second stage of the gasification process, the oxidation of the char obtained in the first stage occurs, and it was developed under isothermal conditions at a temperature of 900 °C for one hour (section 2.4). The TGA and DTG curves of char oxidation as a function of time are shown in Fig. 5a) and Fig. 5b), respectively. For all runs, it is observed that the oxidation of the char occurs during the first 10 min once this stage has started, being slightly lower in the catalytic processes. Therefore, although the second gasification stage was carried out for 60 min, 10 min will be sufficient to achieve total oxidation of the char.

In the four experiments carried out, it can be observed that the process of gasification of the biomass with the support (PS + P) and with the catalysts (PS + Ni/P and PS + Ce/P) results in the oxidation of the char in a shorter time. In Fig. 5 is observed that the highest percentages of weight loss correspond to the PS, this may be because the Pumice is an inorganic material with high thermal stability as reflected in Fig. 2c, remaining in the residue at the end of the process. With respect to the loss of weight that is generated in the PS + Ni/P and PS + Ce/P tests, and in the PS + P test, it can be noted that the catalysts Ni/Pumice and Ce/Pumice are more reactive than the Pumice and, therefore, produces a greater weight loss of the char.

The gas, liquid and solid (char) produced in the pyrolysis process react with the oxidizing agent (air) to produce gases (mainly H_2, CO and CO_2) and smaller amounts of hydrocarbons and olefins. Char gasification is the interactive combination of several gas–solid and gas–gas reactions in which the solid is oxidized to CO and CO_2, and H_2 is produced by the water–gas shift reaction. Gas-solid reactions are the slowest, limiting the overall speed of the process (Castells, 2005). Therefore, char conversion (X), reactivity and gasification rate are important parameters to characterize the gasification process. The more reactive the char, the faster the gasification step will be. Fig. S1, Fig. S2 and Fig. S3 (Supplementary material) show the conversion profiles versus time, the reactivity, the gasification rate of the chars, respectively, of the studied biomass in the gasification process for the four experiments carried out.

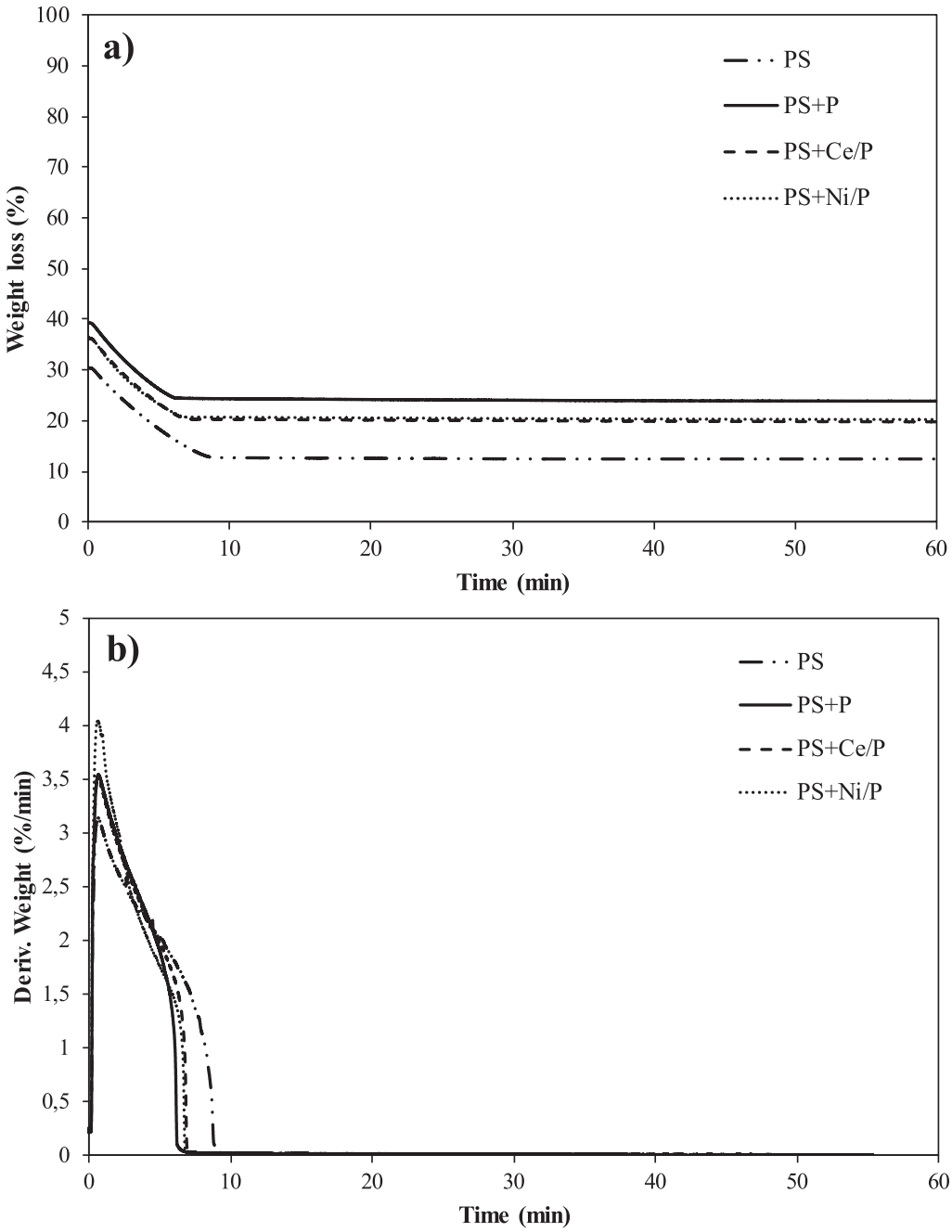

Fig. 5. TGA (a) and DTG (b) curves of the second gasification stage.

Times to reach 50 and 95 % of char conversion (x_{50} and x_{95}, respectively) and reactivity at 50 % of char conversion (R_{50}) for the four experiments are shown in Table S3 (Supplementary material). These parameters allow to analyze the effect of the catalysts during the gasification process. It can be seen in Table S3 and Fig. S1 a) that the time to achieve 50 % and 95 % of conversion is longer for the non-catalytic gasification process (PS). However, the catalytic processes present similar times; consequently, the reactivities R_{50} of catalytic processes were similar (0.34–0.38 min^{-1}) and higher than that of the non-catalytic process (0.28 min^{-1}). Moreover, for conversions around 95 %, the incorporation of the catalyst in the gasification process increases the reactivity of the char (Fig. S2 b) and, as a result, the gasification rate (Fig. S3).

The char conversion is a complex process in comparison with the devolatilization one. The reactivity of char could be influenced by the chemical structure and porosity of the biomass since the char conversion is a heterogeneous process in which chemical reactions take place on the surface (Di Blasi, 2009; Jayaraman and Gökalp, 2015). The influence of biomass type on the char gasification could be related to its inorganic content as opposed to its molecular constituents (cellulose, hemicellulose and lignin) (Dahou et al., 2018).

3.4. Future perspectives

For future studies, several agricultural and forestry biomasses will be studied, as well as the variation of the percentage by weight of the catalyst with respect to the weight of the biomass, and the determination of the activation energy. In addition, it is necessary to carry out the experiments in a pilot plant gasifier to study the reproducibility in the scale-up. Moreover, biomass gasification integrated with CO_2 capture

using CaO sorbent have been successfully used for several authors to reduce CO_2 content and improve H_2 concentration and LHV of the syngas (Rahma et al., 2021). Integration of *Pennisetum setaceum* gasification with CO_2 capture using CaO sorbent could be studied as an alternative treatment to reduce the CO_2 content in the syngas and improve H_2 concentration.

Catalytic biomass gasification is a promising technology for renewable and sustainable energy production that can contribute to several Sustainable Development Goals (SDGs). Some examples of how catalytic biomass gasification can contribute to the SDGs are:

SDG 7: Affordable and Clean Energy - Catalytic biomass gasification can produce syngas can be used to generate electricity and heat in a sustainable and clean way. Furthermore, catalytic gasification of biomass can reduce dependence on fossil fuels.
SDG 9: Industry, innovation and infrastructure - Catalytic biomass gasification is an innovative technology that can provide new opportunities for research and development of renewable energy technologies, as well as for the creation of green jobs. In addition, the production of chemical products from the syngas produced by the catalytic gasification of biomass can be a sustainable alternative to petrochemicals.
SDG 13: Climate Action - Catalytic biomass gasification reduces greenhouse gas emissions by producing energy and chemicals from renewable biomass instead of non-renewable fossil fuels.

4. Conclusions

The energetic properties of *Pennisetum setaceum* from the Canary Islands were studied to know their utilization potential as solid biofuels. *Penisetum setaceum* has relatively low moisture content, high volatile matter content, and low sulfur and nitrogen content, making it a suitable feedstock for thermochemical processes. It has a heating value of 15.1 MJ kg^{-1} and a density of 1517.5 kg m^{-3}, which are within the range of other biomass samples. Its low ash content is desirable for thermochemical processes, as high ash content can lead to severe agglomeration, fouling, and corrosion. Overall, the results suggest that *Penisetum setaceum* is a viable option for energy conversion through thermochemical processes.

The catalyst characterization showed that all the pumitic materials used in the study are mesoporous solids (6.504–18.108 nm), which provided abundant reaction centers for the gasification process. The TGA analysis revealed the catalysts Ce/Pumice and Ni/Pumice have a high thermal stability, above 1000 °C.

The results showed that during the catalytic gasification process of the *Pennisetum setaceum*, the incorporation of the metal (Ce and Ni) on the pumitic material accelerated the decomposition of the hemicellulose, cellulose and lignin contained in the biomass, faster that when Pumice was used. In addition, the gases produced (H_2, CO_2, CH_4 and H_2O) appear at lower temperatures in the catalytic process (641 °C) that in the non-catalytic process (697 °C). The Ce/Pumice catalyst was the one that showed the highest catalytic activity for the reaction due to its higher S_{BET} and higher mesoporosity (18.108 nm); although the results obtained were very close to those obtained with the Ni/Pumice catalyst. Moreover, the incorporation of the catalyst in the gasification process increased the reactivity of the char. The reactivity at 50 % of char conversion for the catalytic process (0.34 and 0.38 min^{-1} for Ce/pumice and Ni/pumice, respectively) was higher than for the non-catalytic process (0.28 min^{-1}), indicating that the incorporation of Ce and Ni on the pumitic material increases the gasification rate of the char compared to the pumitic support.

The catalytic conversion of *Pennisetum Setaseum* with Ce/Pumice and Ni/Pumice is an efficient method for biomass gasification because lower temperatures are required to obtain the syngas compared to non-catalytic gasification. The use of catalysts such as Ni/Pumice and Ce/Pumice would reduce the operating temperatures of a gasifier. In addition, the catalysts presented high thermal stability and are low-cost catalysts.

Declaration of Competing Interest

The authors declare that they have no known competing financial interests or personal relationships that could have appeared to influence the work reported in this paper.

Data availability

Data will be made available on request.

Acknowledgements

This research has been co-funded by FEDER funds. INTERREG MAC 2014-2020 programme within the ACLIEMAC project (MAC2/3.5b/380) and by “Fundación CajaCanarias” and “Fundación Bancaria “la Caixa”” through the “Convocatoria Proyectos Investigación 2019”. Authors would like also to acknowledge to the General Service Research Support of the Universidad de La Laguna for their instrumental and technical support.

Appendix A. Supplementary material

Supplementary data to this article can be found online at https://doi.org/10.1016/j.wasman.2023.05.017.

References

Arias, D., 2018. Plantaciones dendroenergéticas y gasificación de biomasa: nuevos desarrollos con marca TEC. Rev. For. Mesoam. Kurú. 15, 1–6. https://doi.org/10.18845/rfmk.v15i1.3848.
Basu, P., 2010. Biomass Gasification and Pyrolysis, Practical Design. Elsevier Inc. ISBN 978-0-12-374988-8. 10.1016/C2009-0-20099-7.
Borges, M.E., Díaz, L., Alvarez-Galván, M.C., Brito, A., 2011. High performance heterogeneous catalyst for biodiesel production from vegetal and waste oil at low temperature. Appl. Catal. B-Environ. 102 (1–2), 310–315. https://doi.org/10.1016/j.apcatb.2010.12.018.
Çakan, A., Kiren, B., Ayas, N., 2022. Catalytic poppy seed gasification by lanthanum-doped cobalt supported on sepiolite. Int. J. Hydrog. Energy. 47 (45), 19365–19380. https://doi.org/10.1016/j.ijhydene.2022.02.073.
Castells, X.E., 2005. Tratamiento y valorización energética de residuos, Ed. Díaz de Santos. ISBN 978-84-7978-694-6.
Channiwala, S.A., Parikh, P.P., 2002. A unified correlation for estimating HHV of solid, liquid and gaseous fuels. Fuel. 281 (8), 1051–1063. https://doi.org/10.1016/S0016-2361(01)00131-4.
Dahou, T., Defoort, F., Thiéry, S., Grateau, M., Campargue, M., Bennici, S., Jeguirim, M., Dupont, C., 2018. The Influence of Char Preparation and Biomass Type on Char Steam Gasification Kinetics. Energies. 11, 2126. https://doi.org/10.3390/en11082126.
Di Blasi, C., 2009. Combustion and gasification rates of lignocellulosic chars. Prog. Energy Combust. Sci. 35, 121–140. https://doi.org/10.1016/j.pecs.2008.08.001.
Díaz, L., 2018. Procesos de catálisis heterogénea para la obtención de biodiésel. Utilización de aceite de Jatropha curcas y aceite de fritura como materias primas. (Tesis Doctoral). Universidad de La Laguna.
García, R., Pizarro, C., Lavín, A.G., Bueno, J.L., 2012. Characterization of Spanish Biomass Wastes for Energy Use. Bioresour. Technol. 103 (1), 249–258. https://doi.org/10.1016/j.biortech.2011.10.004.
Hernández, M.C., 2019. Gasificación catalítica de biomasa para la producción sostenible de hidrógeno (Tesis doctoral). Universidad Politécnica de Valencia.
Hu, J., Jia, Z., Zha, S., Wan, W., Zhang, Q., Liu, R., Huang, Z., 2021. Activated char supported Fe-Ni catalyst for syngas production from catalytic gasification of pine wood. Bioresour. Technol. 340, 125600 https://doi.org/10.1016/j.biortech.2021.125600.
Jayaraman, K., Gökalp, I., 2015. Pyrolysis, combustion and gasification characteristics of miscanthus and sewage sludge. Energy Convers. Manag. 89, 83–91. https://doi.org/10.1016/j.enconman.2014.09.058.
Khan, M.M., Xu, S., Wang, C., 2022. Catalytic biomass gasification in decoupled dual loop gasification system over alkali-feldspar for hydrogen rich-gas production. Biomass Bioenergy. 161, 106472 https://doi.org/10.1016/j.biombioe.2022.106472.
Kumar Ghodke, P., Kumar Sharma, A., Jayaseelan, A., Gopinath, K.P., 2023. Hydrogen-rich syngas production from the lignocellulosic biomass by catalytic gasification: A state of art review on advance technologies, economic challenges, and future prospectus. Fuel. 342, 127800 https://doi.org/10.1016/j.fuel.2023.127800.
Liu, C., Chen, D., Tang, Q., Abuelgasim, S., Xu, C., Wang, W., Luo, J., Zhao, Z., Abdalazeez, A., Zhang, R., 2023. Chemical looping gasification of biomass char for

hydrogen-rich syngas production via Mn-doped Fe_2O_3 oxygen carrier. Int. J. Hydrog. Energy. 48 (34), 12636–12645. https://doi.org/10.1016/j.ijhydene.2022.12.190.
López-González, D., Fernández-López, M., Valverde, J.L., Sanchez-Silva, L., 2013. Thermogravimetric-mass spectrometric analysis on combustion of lignocellulosic biomass. Bioresour. Technol. 143, 562–574. https://doi.org/10.1016/j.biortech.2013.06.052.
Manić, N.G., Janković, B.Z., Stojiljković, D.D., Jovanović, V.V, Radojević, M.B., 2019. TGA-DSC-MS analysis of pyrolysis process of various agricultural residues. Thermal Sci. 23(5):S1457-S1472. https://doi.org/10.2298/TSCI180118182M.
Manikandan, S., Vickram, S., Sirohi, R., Subbaiya, R., Yedhu Krishnan, R., Karmegam, N., Sumathijones, C., Rajagopal, R., Woong Chang, S., Ravindran, B., Kumar Awasthi, M., 2023. Critical review of biochemical pathways to transformation of waste and biomass into bioenergy. Bioresour. Technol. 372, 128679 https://doi.org/10.1016/j.biortech.2023.128679.
Maurya, R., Gohil, N., Nixon, S., Kumar, N., Noronha, S.B., Dhali, D., Trabelsi, H., Alzahrani, K.J., Reshamwala, S.M.S., Kumar Awasthi, M., Ramakrishna, S., Singh, V., 2023. Rewiring of metabolic pathways in yeasts for sustainable production of biofuels. Bioresour. Technol. 372, 128668 https://doi.org/10.1016/j.biortech.2023.128668.
Mettanant, V., Basu, P., Butler, J., 2009. Agglomeration of biomass fed fluidized bed gasifier and combustor. Can. J. Chem. Eng. 87, 656–684. https://doi.org/10.1002/cjce.20211.
Mujtaba, M., Fernandes Fraceto, L., Fazeli, M., Mukherjee, S., Maira Savassa, S., Araujo de Medeiros, G., Espírito Santo Pereira, A., Donnini Mancini, S., Lipponen, J., Vilaplana, F., 2023. Lignocellulosic biomass from agricultural waste to the circular economy: a review with focus on biofuels, biocomposites and bioplastics, J. Clean. Prod. 402, 136815. 10.1016/j.jclepro.2023.136815.
Murillo, S.E.P., Galán, J.E.L., 2020. Desarrollo sostenible y oportunidad de aprendizaje de las biorrefinerías: Una alternativa de la biomasa. Rev. de Cienc. Soc. 26 (2), 401–413. https://doi.org/10.31876/rcs.v26i0.34135.
Neves, D., Thunman, H., Matos, A., Tarelho, L., Gómez-Bareac, A., 2011. Characterization and prediction of biomass pyrolysis products. Prog. Energy Combust. Sci. 37, 611–630. https://doi.org/10.1016/j.pecs.2011.01.001.
Obernberger, I., Thek, G., 2004. Physical characterisation and chemical composition of densified biomass fuels with regard to their combustion behaviour. Biomass Bioenergy. 27, 653–669. https://doi.org/10.1016/j.biombioe.2003.07.006.
Özsin, G., Pütün, A.E., 2017. Kinetics and evolved gas analysis for pyrolysis of food processing wastes using TGA/MS/FT-IR. Waste Manage. 64, 315–326. https://doi.org/10.1016/j.wasman.2017.03.020.
Parascanu, M.M., Sandoval-Salas, F., Soreanu, G., Valverde, J.L., Sánchez-Silva, L., 2017. Valorization of Mexican biomasses through pyrolysis, combustion and gasification processes. Renew. Sustain. Energy Rev. 71, 509–522. https://doi.org/10.1016/j.rser.2016.12.079.
Rahma, F.N., Tamzysi, C., Hidayat, A., Adnan, M.A., 2021. Investigation of Process Parameters Influence on Municipal Solid Waste Gasification with CO_2 Capture via Process Simulation Approach. Int. J. Renew. Energy Dev. 10(1):1-10. https://doi.org/10.14710/ijred.2021.31982.
Ren, J., Cao, J., Zhao, X., Yang, F., Wei, X., 2019. Recent advances in syngas production from biomass catalytic gasification: A critical review on reactors, catalysts, catalytic mechanisms and mathematical models. Renew. Sustain. Energy Rev. 116, 109426 https://doi.org/10.1016/j.rser.2019.109426.
Rodríguez Martínez, E.D., 2009. Eficiencia de activadores alcalinos basados en diferentes fuentes de sílice para la producción de sistemas geopoliméricos de cenizas volante. Trabajo de investigación CST/MIH-05, Universidad Politécnica de Valencia.
Singh, R., Hans, M., Kumar, S., Yadav, Y.K., 2023. Thermophilic Anaerobic Digestion: An Advancement towards Enhanced Biogas Production from Lignocellulosic Biomass. Sustainability. 15 (3), 1859. https://doi.org/10.3390/su15031859.
Swierczynski, D., Libs, S., Courson, C., Kiennemann, A., 2007. Steam reforming of tar from a biomass gasification process over Ni/olivine catalyst using toluene as a model compound. Appl. Catal. B Environ. 74, 211–222. https://doi.org/10.1016/j.apcatb.2007.01.017.
Temuujin, J., Okada, K., Mackenzie, K., 2002. Preparation and properties of potassium aluminosilicate prepared from the waste solution of selectively leached calcined kaolinite. Appl. Clay. Sci. 21 (3–4), 25–131. https://doi.org/10.1016/S0169-1317(01)00082-5.
Tulu, T.K., Atnaw, S.M., Bededa, R.D., Wakshume, D.G., Ancha, V.R., 2002. Kinetic Modeling and Optimization of Biomass Gasification in Bubbling Fluidized Bed Gasifier Using Response Surface Method. Int. J. Renew. Energy Dev. 11(4):1043-1059. https://doi.org/10.14710/ijred.2022.45179.
UNE-EN ISO 18122:2016, Biocombustibles sólidos. Determinación del contenido de ceniza. AENOR, Madrid.
UNE-EN ISO 18123:2016, Biocombustibles sólidos. Determinación del contenido en materia volátil. AENOR, Madrid.
UNE-EN ISO 18134:2016, Biocombustibles sólidos. Determinación del contenido de humedad. Método de secado en estufa. Parte 1: Humedad total. Método de referencia. AENOR, Madrid.
Wang, J., Zhang, S., Xu, D., Zhang, H., 2022. Catalytic activity evaluation and deactivation progress of red mud/carbonaceous catalyst for efficient biomass gasification tar cracking. Fuel. 323, 124278 https://doi.org/10.1016/j.fuel.2022.124278.
Yang, H.P., Yan, R., Chen, H.P., Lee, D., Zheng, C.G., 2007. Characteristics of hemicellulose, cellulose and lignin. Fuel. 86, 1781–1788. https://doi.org/10.1016/j.fuel.2006.12.013.
Zhang, Z., Liu, L., Shen, B., Wu, C., 2018. Preparation, modification and development of Ni-based catalysts for catalytic reforming of tar produced from biomass gasification. Renew. Sustain. Energy Rev. 94, 1086–1109. https://doi.org/10.1016/j.rser.2018.07.010.